ELSEVIER

Chemical Engineering Journal 137 (2008) 386–395

Chemical Engineering Journal

www.elsevier.com/locate/cej

Mixing and hydrodynamics investigation using CFD in a square-sectioned torus reactor in batch and continuous regimes

Laura Pramparo [a], Jeremy Pruvost [c], Frank Stüber [a], Josep Font [a], Agustí Fortuny [b], Azael Fabregat [a], Patrick Legentilhomme [c], Jack Legrand [c], Christophe Bengoa [a,*]

[a] *Department of Chemical Engineering, Escola Tècnica Superior d'Enginyeria Química, University Rovira i Virgili, Països Catalans 26, 43007 Tarragona, Spain*

[b] *Department of Chemical Engineering, Escola Tècnica Superior d'Enginyeria Química, University Politècnica de Catalunya, Víctor Balaguer, 08800 Vilanova i la Geltrú, Spain*

[c] *GEPEA, UMR-CNRS 6144, Université de Nantes, CRTT, B.P. 406, F-44602 Saint-Nazaire Cédex, France*

Received 10 October 2006; received in revised form 3 April 2007; accepted 2 May 2007

Abstract

The goal of this work was the study of the flow in a square-sectioned torus reactor, in both batch and continuous conditions. A characterization of hydrodynamics in the reactor by computational fluids dynamics (CFD) using Fluent software® is presented. Results obtained in batch conditions for the mean bulk velocity as a function of the impeller rotation speed are studied and are compared to a correlation available for a circular-sectioned torus reactor. Mixing time is also investigated. The study is next extended to the case of the continuous regime. After validation of the residence time distribution (RTD) by experimental determination, the influence of the inlet–outlet flowrate on the hydrodynamic characteristics is established, emphasizing a possible modification of mixing performance of the reactor when conducted in continuous mode, depending on the ratio of the circulation time to the mean residence time.

Keywords: Torus reactor; Batch; Continuous; Hydrodynamics; Mixing; Computational fluid dynamics

1. Introduction

The torus reactor is considered as a loop reactor. Owing to its configuration, it presents several advantages compared with the stirred tank reactor including an efficient mixing of the reactants, an easy scale-up due to the absence of dead volume, low power consumption [1], good high heat transfer capacity [2], prevention of deposition of polymer or biomaterial on the reactor wall and high efficiency [1,3,4]. These advantages make the torus reactor as a promising alternative to more classical configurations.

Some studies have shown the interest of the torus reactor for its application in processes using viscous fluids and as a bioreactor in two-phase systems. Hosogai and Tanaka [5] used a circular loop reactor for the polymerization in suspension of styrene. They have shown that this reactor is more efficient for the production of uniform size particles than the conventional stirred reactor. Laederach and Widmer [6] tested the torus reactor in batch conditions for the growth of a fermentating culture. With this reactor, the biomass production was around 40% higher than that obtained using a stirred reactor. Adler and Fiechter [7] have assessed different types of bioreactors with the help of a microbiologic growth test system. They have shown the interest of the torus reactor with regard to the stirred one for systems subjected to a foam formation. They also showed that, for this application, the extrapolation of the results obtained with a stirred reactor is not possible. Nouri et al. [1] have studied the enzymatic application of the torus reactor in the hydrolysis of wheat proteins. The performance comparison with that of the stirred one has been carried out using a volumetric power criterion and the hydrolysis degree. The authors have shown that, for a limited hydrolysis of the wheat proteins, difference in reactors performance is not significant, but the process in the stirred reactor was perturbated by the formation of high amounts of foam that was not detected in the torus reactor. Legrand et al. [3] have analyzed the pea acetylation in a torus minireactor, which was particularly suited to this biochemical reaction. Belleville et al. [8] have shown that the torus reactor in batch conditions presents an efficient radial mixing inducing little dead volumes and allowing an

* Corresponding author. Tel.: +34 977 558619; fax: +34 977 559621.
E-mail address: christophe.bengoa@urv.cat (C. Bengoa).

1385-8947/$ – see front matter © 2007 Elsevier B.V. All rights reserved.
doi:10.1016/j.cej.2007.05.013

Nomenclature

C	concentration (mol m^{-3})
CFD	computational fluids dynamics
C_{final}	average final concentration in the reactor (mol m^{-3})
$C_T(t)$	tracer concentration (mol m^{-3})
D_j	axial dispersion coefficient of j species (m^2 s^{-1})
D_t	reactor diameter (m)
F_g	geometrical parameter of the impeller
L_x	reactor length in the axial coordinate (m)
L_y	reactor length in curvilinear coordinate (m)
L_z	reactor average length (m)
MRF	multiple reference frame
N	rotation velocity of the impeller (rpm)
PMMA	polymethyl methacrylate
Q	flow rate (ml h^{-1})
Re	Reynolds number
R_t	bend curvature radius (m)
RTD	residence time distribution (s)
Sc	Schmidt number
t	mean residence time (s)
t_c	circulation time (s)
t_c	mean circulation time (s)
T_m^*	dimensionless mixing time
U	axial velocity component (m s^{-1})
U_0	mean bulk velocity (m s^{-1})
V	reactor volume (l)
x	axial coordinate (m)
y	wall distance (m)
z	longitudinal coordinate (m)

easier scale-up of the results. Benkhelifa et al. [4] have studied the casein hydrolysis by immobilized enzymes in a batch torus reactor. This work shows promising results in the use of the torus reactor in bioprocesses involving immobilized enzymes.

Despite experimental studies have confirmed efficiency of the torus geometry, the optimal conception of torus reactors and their utilization in industrial scale production require still theoretical research. Few informations about hydrodynamic characteristics involved in torus shape reactors are known. Khalid et al. [9,10] emphasize the main features of the flow, and especially the high degree of mixing and the decay of the swirling motion when moving far from the impeller zone.

Other studies are mainly restricted to global measurements, like the circulation time as a function of the impeller rotation speed [2], or a general overview of the flow structure using tracer methods [11]. This is mainly explained by the difficulties encountered to conduct an experimental investigation of the complex flow obtained in torus geometries. But because the resulting hydrodynamics complexity also explains reactor efficiency, such kind of investigations is of primary interest.

The flow modelling of a circular-sectioned toroidal reactor in batch and continuous operating modes was studied by Benkhelifa et al. [12] using a reactor with a volume of 5.25 l. They determined the tracer evolution in batch system and residence time distribution in continuous mode. The flow in the reactor has been modelled with a plug flow with axial dispersion and total or partial recirculation in order to determine the axial dispersion coefficient in the reactor and to optimize the other experimental parameters such as the mean circulation time and the recycling factor. The determination of the Péclet number showed that the axial dispersion coefficient in the torus reactor is nearly constant whatever the operating mode and the flow regime. The axial dispersion is close to that obtained in vortex flows which are characterized by well-defined flow structures [13] and allows good mass and heat transfers. However, despite its interest in reactor running modelling, especially when reactions are occurring, such kind of investigation gives only a general representation of the flow in the geometry.

In this context, CFD appears as an interesting tool to conduct a further analysis of flow structures. The modelling of the entire flow in torus reactor is however not easy, because of the combined effects of the bend curvature and the impeller rotation. Interaction between the helical motions with Dean vortices can be strong, as shown in Pruvost et al. [14] in a numerical study of the flow in a U-bend using the commercial code Fluent. In Pruvost et al. [15], numerical investigation is extended to the case of the torus reactor geometry. This study is devoted to a numerical analysis of the particular flow conditions involved in a torus geometry, and especially the competition between the swirling motion, due to the impeller rotation, with Dean vortices generated in bends. Results achieved with the commercial code Fluent being satisfactory, same authors [16] have also applied CFD to the particular case of a square-sectioned photobioreactor of torus geometry. Relevant characteristics for this application were investigated, like mixing time, radial mixing and shear stress. But it must be noticed that only batch configuration was considered.

When operated in continuous mode, mixing performance can be modified [12], due to flow inlet and outlet that can alter the flow structure inside the reactor. This is obviously a function of the feeding flowrate, and thus of the residence time in the reactor. The aim of the present study is to characterize the flow behaviour of a square-sectioned torus reactor in continuous and batch conditions, by combining both experimental and numerical approaches. For the continuous mode, simulations are validated with experimental residence time distribution determination. Next, CFD is employed to explain reactor behaviour by numerically investigating the flow structure. The study is finally focused on the perturbation occurring in continuous mode for high feeding flowrates.

2. Experimental investigation in continuous conditions

2.1. Torus reactor: experimental set-up

The torus reactor is presented in Fig. 1a. The reactor has a square section with a side width $L_x = L_y = D_t = 25$ mm, a mean bend curvature $R_t = 25.5$ mm and a loop length of 160 mm (L_z), giving a reactor volume of 100 ml. The reactor is manufactured in poly(methyl-methacrylate) (PMMA) and is transparent.

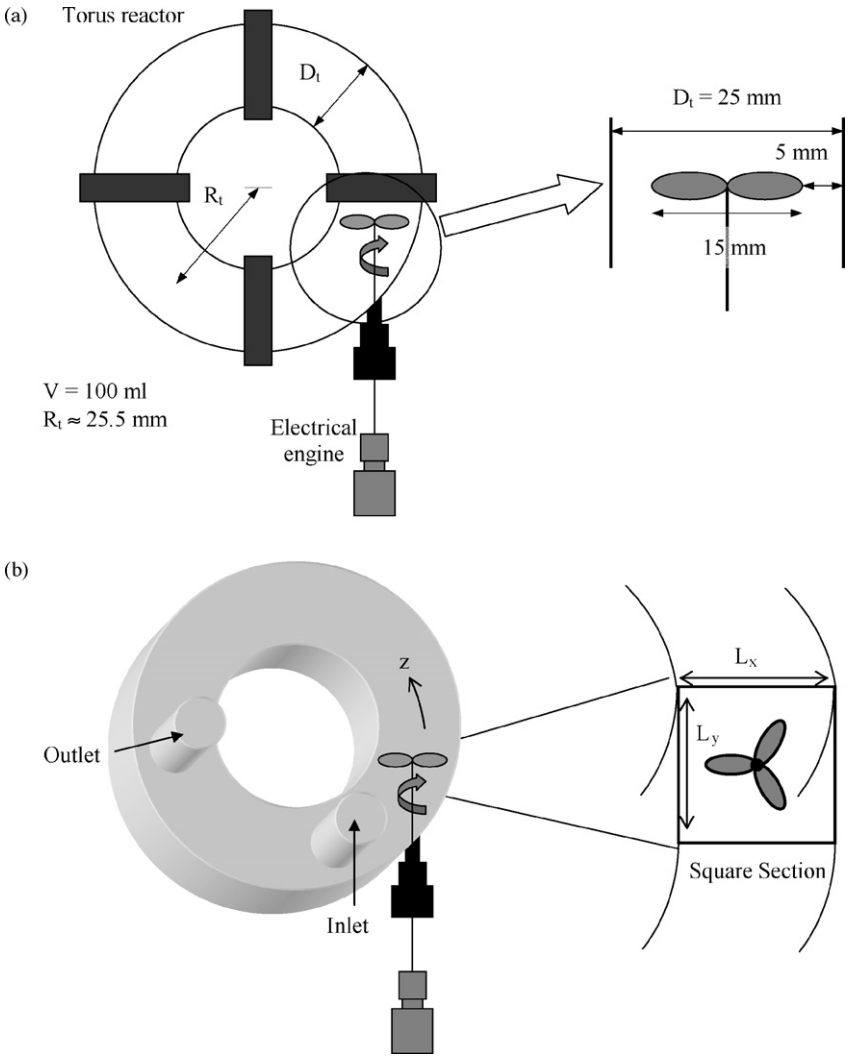

Fig. 1. (a) Schematic representation of the torus reactor. (b) Continuous torus reactor (showing inlet and outlet lines).

Agitation into the reactor is achieved by a three blades marine impeller with a blade pitch angle of 45° and an external diameter of 15 mm. An electrical engine of variable velocity controlled by a tachymeter (Heidolph model RZR 2021) was used to control the rotation of the impeller.

2.2. Residence time distribution measurements

The RTD depends of the flow hydrodynamics and of the reactor geometry, and has an influence on the reactor chemical performances (conversion, yield, ...). It is thus a fundamental concept in reactor design. The determination of the residence time distribution is carried out by measuring evolution of a tracer concentration using a conductimetric method. A two-points detection method is used, allowing the measurement of the concentration evolutions at both inlet and outlet of the reactor.

The hydraulic circuit is constituted by a vessel containing feed water, a moto-pump Stepdos 08RC (Knf Flotdos) and the inlet and outlet lines. The inlet tube is located at a distance of z/L_z between 0.75 and 0 (in reference with the impeller) and the outlet tube is located at $z/L_z = 0.5$ as it can be seen in Fig. 1b. The two conductimetric probes are identical and constituted both by two hemicylindrical nickel sheets. Each probe is connected to a variable frequency conductimeter (Tacussel CD810). An operating frequency of 16,000 Hz was adopted in order to avoid the polarization of the electrodes and also to ensure a linear relationship between the conductivity and the tracer concentration. Both concentration signals, obtained at the inlet and at the outlet of the reactor, respectively, are sampled using an AOIP model SA32 data acquisition device, connected to a personal computer (PC).

Demineralized water is used as working fluid. A solution of sodium chloride (4 N) is used as tracer. A small quantity (1 ml) of tracer is injected with a syringe in the inlet tube to simulate a pulse and do not disturb the flow inside the reactor. The obtained outlet curve and its comparison to the inlet one allows the estimation of the mean residence time. Different operating conditions have been tested, as an impeller rotation velocity N of 500, 1000, 1500 and 1800 rpm and also different flow rates, Q, ranged between 180 and 1200 ml h^{-1}.

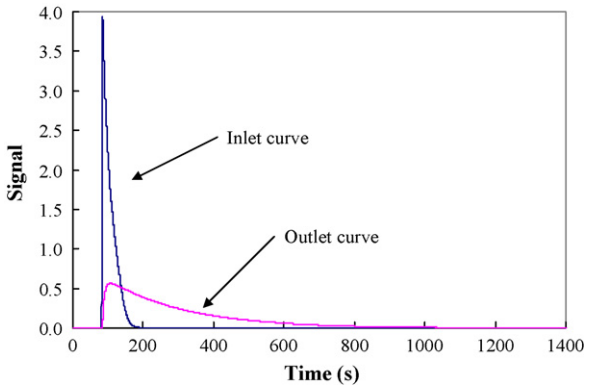

Fig. 2. Typical response of the conductimetric method: inlet and outlet signals ($N = 1500$ rpm, $Q = 1200$ ml h^{-1}).

2.3. Results

Fig. 2 shows an example of the curves obtained at the inlet and at the outlet of the reactor. These curves were obtained for $N = 1500$ rpm and $Q = 1200$ ml h^{-1} ($Re = 7200$, see definition in Section 4.1) and are representative of all tested experimental conditions. The experimental mean residence times were obtained using the conductimetric method. When the flowrate increases, the residence time decreases quickly. For incompressible flows, the mean residence time must satisfy $\tau = V/Q$, and is thus independent of the impeller rotation speed. Comparison with values obtained experimentally gives an estimation of the accuracy of the experimental determination, some differences being observed for same flow rates but different impeller rotation speeds. There is thus a lack of precision in the calculation, especially for small flow rates and small rotation speeds, the residence time of the tracer being in these cases very dispersed.

3. Numerical simulation

3.1. Introduction

The hydrodynamic characterization of the torus reactor in both batch and continuous conditions was carried out with numerical simulation using the commercial code Fluent® (Fluent Inc.). The first step in numerical simulation is to create the reactor geometry and to mesh it. The torus shape was three-dimensionally meshed using the Gambit Software® (Fluent Inc.). Due to the impeller, a regular mesh is difficult to apply in the entire geometry. So, the reactor was divided in two different zones. The first one, in the marine impeller vicinity has been meshed using tetrahedral volumes and prisms. A regular mesh with elementary hexahedral volumes has been used in the remaining part of the torus. The grid discretization in this regular part is uniform, whereas cells density is gradually increased when coming closer to the impeller. To mesh the region near the impeller, a refinement function (named "size function" in Fluent) is applied to control the cells density in boundary layers. This function determines the size of the first near-wall elementary volume and the discretization step.

The motion of the impeller was modelled using the multiple reference frames (MRF) resolution, the description of which can be found in Brucato et al. [17] and its utilization in the torus geometry in Pruvost et al. [15]. The flow-field was obtained using the k–ω turbulence model (see Wilcox [18] for detail). This model was found to give good results for torus geometry [14,15,16]. Boundary layers were meshed using a standard wall-function approach, as in Pruvost et al. [16], with an appropriate meshing in the wall region.

3.2. Reactor in batch conditions

To ensure grid independency of the results, three meshes (301,473, 338,973 and 348,531 cells) have been tested. These results showed that the data of flow velocities were totally independent of the number of cells of the grid.

In the batch configuration, the torus reactor was considered closed (no inlet or outlet conditions are applied) and the flow is only driven by the impeller rotation. The only boundary condition to be specified in this case was the rotation speed of the impeller.

The mixing performance in the torus reactor was numerically evaluated by determining the mixing time. This is obtained by the simulation of a pulse tracer injection. In the case of turbulent flows, the diffusion process has to be taken into account by means of the turbulent mass diffusivity D_{jt}, expressed by the turbulent Schmidt number. The value in turbulent flow for the Schmidt number is set to $Sc_t = 1$ as described by Pruvost et al. [15]. The tracer dispersion is next determined by solving the unsteady formulation of the mass transport equation. Because the tracer injection is considered to not influence the flow, the steady solution of the flow-field inside the reactor can be used (only mass transport is solved with an unsteady resolution). The injection was located at a distance $Z_{imp} = z/L_z = 0.25$ from the impeller as it can be seen in Fig. 3. In the unsteady resolution of the tracer transport, evolution with respect to time of tracer concentration averaged on a given cross-section allows to determine the mixing time. This cross-section was located at the same distance from the impeller used for the injection point.

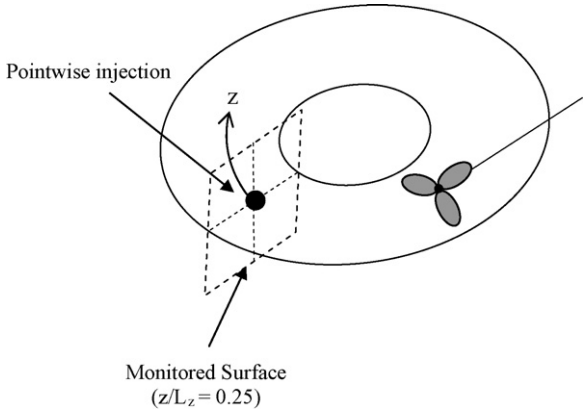

Fig. 3. Passive tracer injection: visualization of the monitored surface and the injection point in batch reactor.

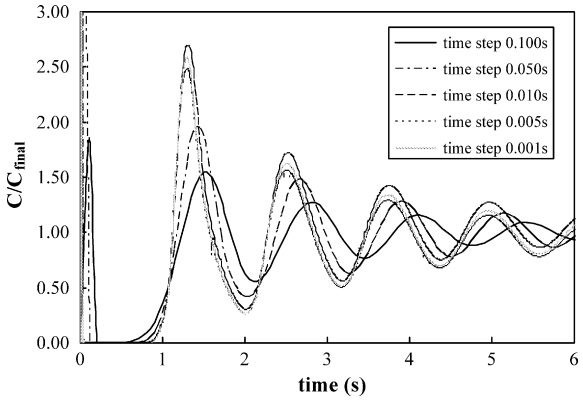

Fig. 4. Time evolution of the normalized concentration averaged on a given flow cross-section ($z/L_z = 0.25$): influence of the time step on the unsteady resolution ($N = 800$ rpm).

For the unsteady resolution of mass transport equation, it is necessary to specify a time step Δt, which has been chosen small enough to ensure accurate results. Different tests have been done to determine the time step effect, as presented in Fig. 4 for $N = 800$ rpm. The tested time step values were 0.100, 0.050, 0.010, 0.005 and 0.001 s. The numerical results show that a time step around 0.005 s can be used. The curves obtained for 0.001 and 0.005 s are indeed very similar. In all calculations, a time step of 0.005 s will be used to save calculation time.

3.3. Reactor in continuous conditions

For the continuous regime, the reactor mesh was modified by introducing pipes for the inlet and outlet flows. The irregular zone which is located near the impeller was meshed in the same way that for the batch conditions. The inlet and outlet zones were meshed using hexagonal/wedge volumes because they were also considered as irregular zones. The resulting grid was composed of 349,981 cells as it can be seen in Fig. 5.

In continuous conditions, hydrodynamics is the result of the impeller rotation and the flowrate applied in the inlet of the reactor. A MRF resolution was then conducted, with investigated flowrates applied in flow inlet as boundary condition.

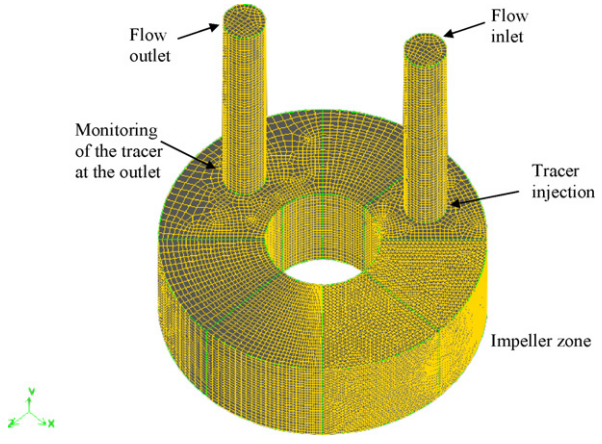

Fig. 5. Continuous torus reactor grid (349,981 cells) and localization of the surface for the simulation of the tracer injection.

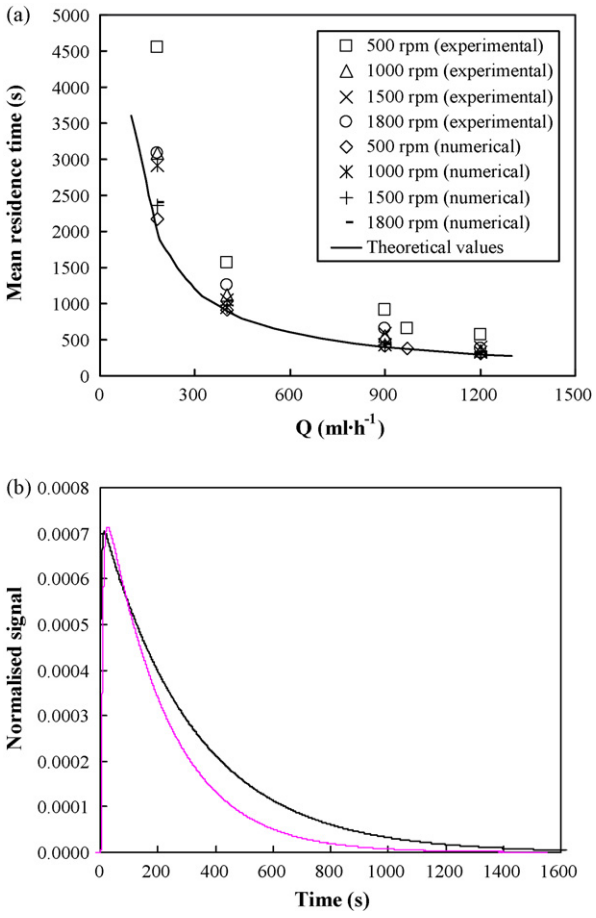

Fig. 6. (a) Experimental and simulated values of the mean residence time. (b) Experimental and numerical prediction of the residence time distribution.

As in batch conditions, the tracer dispersion was solved using mass-transport equation. To simulate the two-point RTD experimental measurement, the passive tracer was introduced as a pulse by changing its concentration in the feed as illustrated in Fig. 5. The averaged tracer concentration was monitored as a function of time at the outlet of the reactor. Results provide the exit age distribution of the tracer between the inlet and the outlet of the reactor, and therefore, represent the RTD.

3.4. Validation in continuous regime

Hydrodynamic simulations in batch regime have already been validated [16]. For the continuous regime, the validation was achieved by comparing simulated RTD to experimental ones. An example of results is given in Fig. 6a, showing agreement between numerical simulations and experimental measurements. As for the experimental characterization, a lack of accuracy is observed for small values of impeller rotation speeds and flow rates, explained by the poor mixing in those conditions, resulting in a very dispersed distribution of exit age of the injected tracer making difficult calculation of the mean residence time. Obviously, the mean residence time is not sufficient to validate the numerical simulation, this value

being fixed by the feeding flow rate and reactor volume only ($\tau = V/Q$). In Fig. 6b is presented the outlet curves achieved numerically and experimentally. The same shape is obtained. The curves are not equivalent but a relative agreement is however observed, considering accuracy of the experimental measurements. It is indeed difficult to obtain an accurate determination of RTD, especially due to its dispersed nature. For a deep investigation of the flow structure, experimental validation by only RTD is not sufficient, because of the global nature of this characteristic (different flow structures can give same RTD). But, considering previous characterization on almost same reactor geometries [16], and the aim of this study that is to have only a global overview of the mixing efficiency in continuous and batch modes, such validation can be considered as sufficient. The numerical procedure has then been retained in the next part of the study.

4. Results of the numerical investigation

4.1. Batch mode

In batch mode, two values are of primary relevance, the circulation velocity U_0 and the mixing time T_m. Results of U_0 are given in Fig. 7. U_0 is deduced from the axial component of velocity (z-direction) by a simple spatial averaging on a cross-section of the reactor. Results are given for impeller rotation velocities varying from 200 to 2000 rpm. As it can be seen in Fig. 7a, the circulation velocity increases with the impeller rotation speed. Those results can be compared to the ones determined experimentally by Belleville et al. [8] and further confirmed by Khalid et al. [9] in a torus reactor with circular section. Belleville et al. [8] established the following correlation:

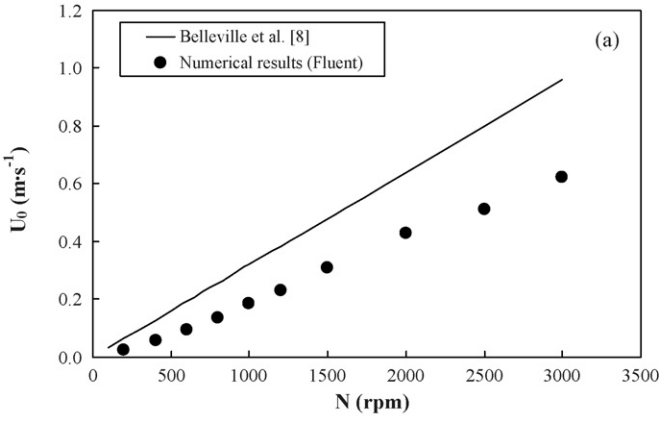

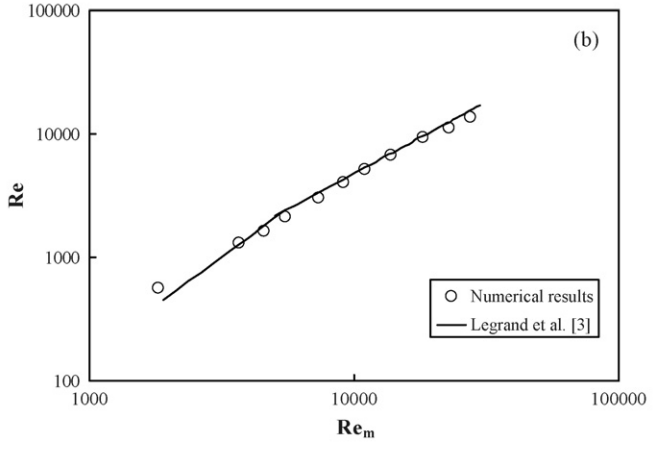

Fig. 7. (a) Mean bulk velocity as a function of the impeller rotation speed: comparison with the empirical correlation of Belleville et al. [8]. (b) Variation of the Reynolds number as function of the mixing Reynolds number.

$$U_0 = 0.06 F_g N \tag{1}$$

where U_0 is the mean bulk velocity, N the rotation speed of the impeller and F_g is a geometric factor defined by:

$$F_g = \frac{d_1^2 - d_2^2}{D^2} tg\phi \tag{2}$$

The parameters d_1 and d_2 are the inner and outer diameters of the impeller, ϕ the pitch angle of the blades and D is the pipe inner radius. In this case, the reactor has a square section and the diameter used in the equation was the hydraulic one. F_g is constant and equal to 0.32.

It must be noticed that the relation between the circulation velocity and the impeller rotation speed is strictly linear, that is in agreement with the correlation presented by Belleville et al. [8]. However, the mean bulk velocity obtained for a fixed impeller rotation speed is even lower in the case of a square-sectioned reactor. As it was described by Pruvost et al. [14], the use of a square-sectioned geometry reduces the induced flow rate in the torus geometry, because the swirling flow is better maintained in circular-sectioned pipes.

This is also interesting to introduce the Reynolds number. In a mixing tank, where there is no bulk velocity, the Reynolds number is given like the mixing Reynolds number $Re_m = \rho N D^2/\mu$. In the torus reactor, the Reynolds number can be considered $Re = \rho U_0 D/\mu$, based in U_0 previous results. In the case of batch torus reactor, the relation between Re and Re_m is given by [3]:

$$Re_m > 4500 - 5500, \quad Re = 0.1109 \cdot Re_m^{1.16} \tag{3}$$

$$Re_m < 4500, \quad Re = 0.0027 \cdot Re_m^{1.59} \tag{4}$$

These equations were obtained for a square-sectioned torus reactor of 0.1 l. Fig. 7b shows the correlations of Reynolds number as a function of the mixing Reynolds number for a torus reactor and also the results obtained by numerical prediction. The results are in agreement with the predicted correlations, especially for Reynolds numbers higher than 1000.

For the torus reactor used in this study, it is possible to obtain a correlation between mixing Reynolds number and Reynolds number. The relationship is given in Eq. (5).

$$Re = 0.0695 \cdot Re_m^{1.2} \tag{5}$$

For our study, if N is ranged between 200 and 3000 rpm, Reynolds numbers are between 550 and 13,700.

The mixing time, T_m, was determined by time monitoring evolution of tracer concentration. Fig. 8 gives an example of time-variation of the concentration for an impeller rotation speed of 1500 rpm. The mean circulation time corresponds

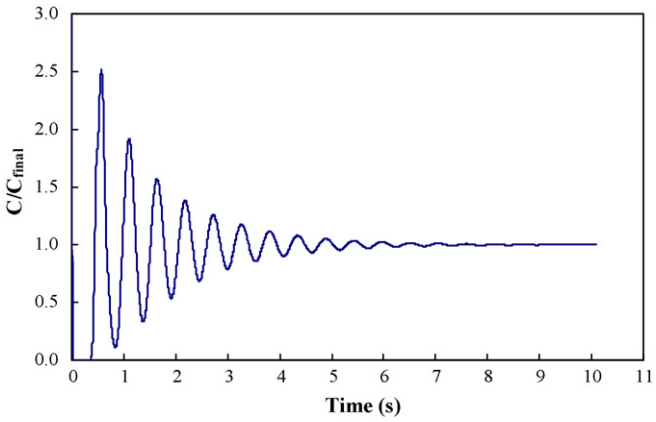

Fig. 8. Example of mixing time determination: time evolution of the normalized concentration averaged on the monitored surface ($z/L_z = 0.25$, $N = 1500$ rpm).

to the time between two consecutive peaks on the response curve. T_m is defined by the time to achieve the final concentration obtained at total dilution, C_{final}, with a variance value of 5%.

Fig. 9 depicts the variation of the mixing time as a function of the impeller rotation speed. As it can be seen, the mixing time decreases rapidly with the increase of the impeller rotation speed. These results are in agreement with those obtained by Benkhelifa et al. [12].

The maximum value of the mixing time is 21 s for an impeller rotation speed of 200 rpm. Even for small impeller rotation speeds, mixing time can be considered sufficiently short to achieve a rapid concentration homogeneity in the reactor.

Another important parameter to be analyzed is the dimensionless mixing time T_m^*, defined by: $T_m^* = N \cdot T_m$ [19]. This allows a comparison with classical geometries, like mixing tanks, where this parameter is found to be independent of the Reynolds number if turbulent regime is achieved [19]. Fig. 10 presents the values of T_m^* for impeller rotation speeds varying from 200 to 2000 rpm. As it can be seen, T_m^* is found to be constant for N greater than 1200 rpm, a classical result in mixing tank, but for this impeller rotation speed, the Reynolds is about 5800. A fully

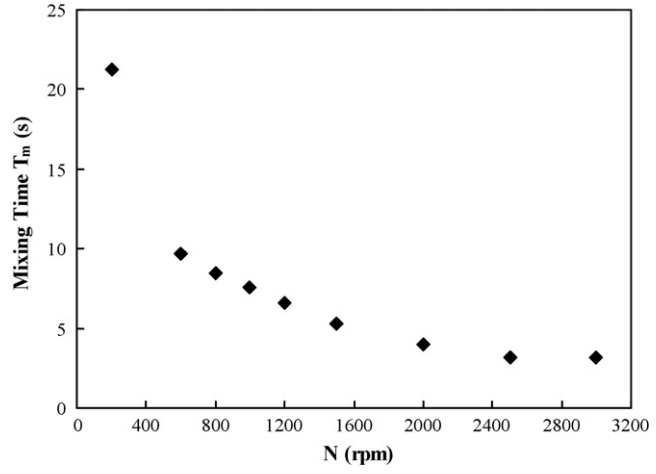

Fig. 9. Mixing time numerical prediction: evolution of the mixing time with the impeller rotation velocity.

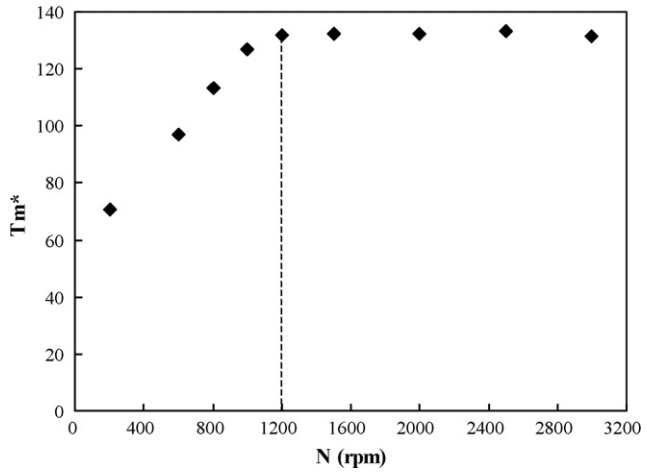

Fig. 10. Mixing time numerical prediction: dimensionless mixing time.

turbulent regime is thus obtained from this value with this kind of reactor.

4.2. Continuous mode

Due to flow inlet and outlet, the continuous regime can lead to different hydrodynamics compared to the batch one. If this is the case, relation between N and U_0 will be modified. Table 1 presents the results obtained for the mean circulation velocities U_0 into the reactor for different impeller rotation speeds ranged from 0 to 2000 rpm and, for different flowrates, varying from 180 to 1200 ml h^{-1}. For all flowrates, results mainly depend on the impeller rotation speed as observed in batch conditions. The differences between batch and continuous conditions are very low as it can be seen in Fig. 11, where both curves have a same behaviour, similar to that presented by Benkhelifa et al. [12]. Only a difference is observed for low rotation speeds. In Fig. 12a is presented the evolution of the ratio of the mean circulation time in continuous conditions, t_{cc}, to the one

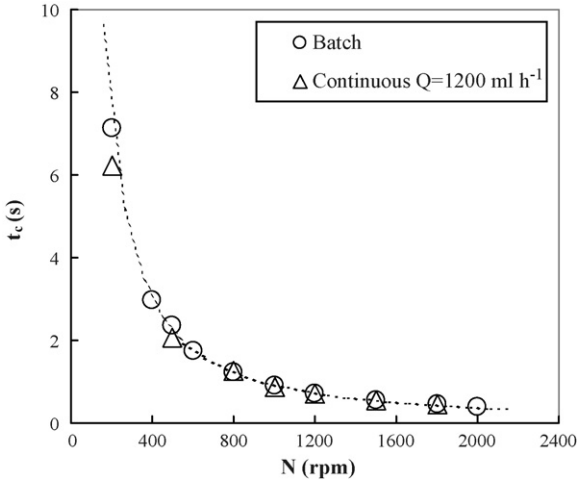

Fig. 11. Mean circulation times obtained for batch and continuous conditions for different impeller rotation speeds and for a flowrate of 1200 ml h^{-1}.

Table 1
Mean circulation velocities ($m\,s^{-1}$) into the reactor for different impeller rotation speeds

Speed, N (rpm)	Condition				
	Batch	Continuous			
		$Q = 180\,ml\,h^{-1}$	$Q = 400\,ml\,h^{-1}$	$Q = 900\,ml\,h^{-1}$	$Q = 1200\,ml\,h^{-1}$
0		0.0002	0.0005	0.0008	0.0012
200	0.0224	0.0256	0.0257	0.0256	0.0258
400	0.0538				
500	0.0744	0.0784	0.0784	0.0782	0.0781
600	0.0915				
800	0.1302				0.1285
1000	0.1766	0.1848	0.1856	0.1850	0.1838
1200	0.2247			0.2322	0.2225
1500	0.2971	0.3024	0.3026	0.3019	0.2919
1800	0.3518	0.3754	0.3754	0.3751	0.3617

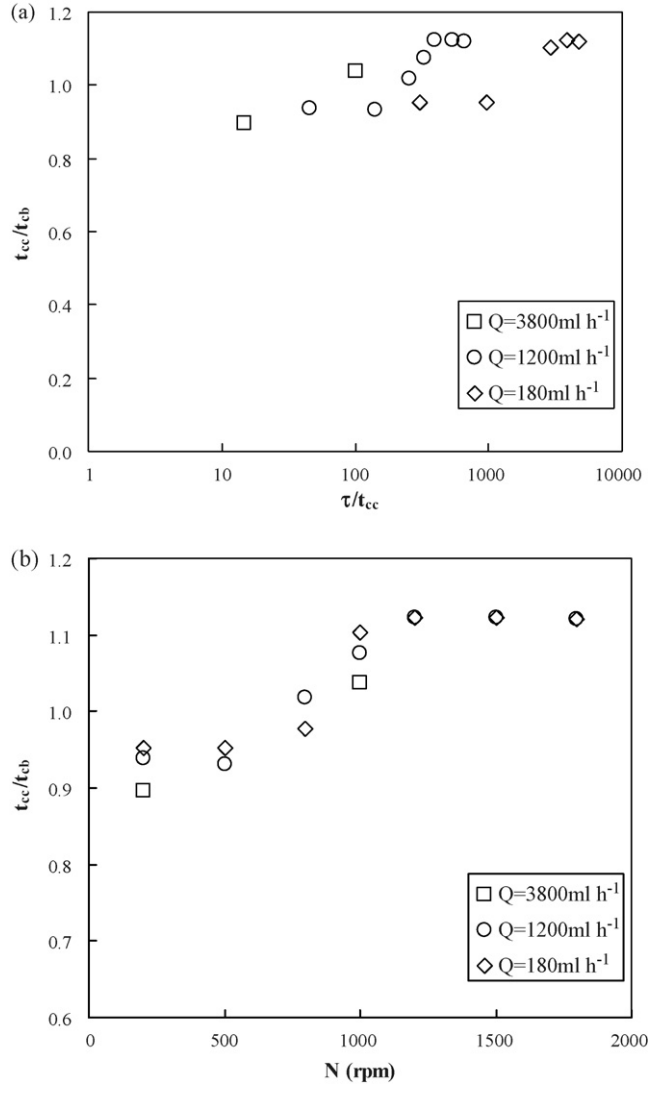

Fig. 12. (a) Comparison of the mean circulation time in continuous and batch conditions as a function of the τ/t_{cc} ratio for different flowrates. (b) Comparison of the mean circulation time in continuous and batch conditions as a function of the impeller rotation speed for different flowrates.

in batch conditions, t_{cb}, as a function of τ/t_{cc} ($\tau = V/Q$). The ratio between the residence time, τ, and the mean circulation time in continuous mode characterizes the importance of the injection flowrate on the circulation. The t_{cc}/t_{cb} ratio is nearly equal to 1.1 for high values of τ/t_{cc} and less than 1 when the rotation speed is low (less than 800–1000 rpm). This indicates that hydrodynamics inside the reactor is perturbed in particular conditions, for small values of N, or for high values of Q, depending of the ratio characterized by τ/t_{cc}. Fig. 12b indicates that N plays a major role. Below a given value of the rotation speed, all feeding flow rates in the continuous system have an influence on the circulation inside the reactor, which is accelerated. This results in a lower mean circulation time, as it was previously reported by Benkhelifa et al. [12]. This phenomenon is particularly important when the value of τ/t_{cc} is smaller than 20 ($t_{cc}/t_{cb} < 0.8$) for Benkhelifa et al. [12]. But in the case under study, this cannot be observed. This is certainly explained by the inlet position which is different. In Benkhelifa et al. [12] case, the inlet injection is in the direction of the flow circulation, favouring the circulation inside the reactor. In our case, the flow inlet is set perpendicular to it and has thus a smaller influence. Depending of the impeller rotation speed, the circulation time inside the reactor can even be increased or decreased. For small value of N, feeding flow rate accelerates the circulation inside the reactor, the contrary (deceleration of the flow circulation) being observed for values of $N > 1000$ rpm. Differences in flow structure due to the inlet flowrate can be seen in Fig. 13. In this figure, it is possible to see the perturbation of the flow on the velocity distributions, which is naturally higher for high feeding flow rates (Fig. 13b), small value giving negligible perturbation (Fig. 13a). For a impeller rotation speed of 200 rpm and a flowrate of $7200\,ml\,h^{-1}$, the ratio t_{cc}/t_{cb} is around 0.88. Despite such operating conditions correspond to an extreme case, influence on the flows structure remains limited. It can thus be concluded that in normal operating conditions as it will be used in further exploitation of the torus reactor (typically $Q < 1200\,ml\,h^{-1}$), reactor hydrodynamics in continuous regime will mainly be the result of impeller rotation.

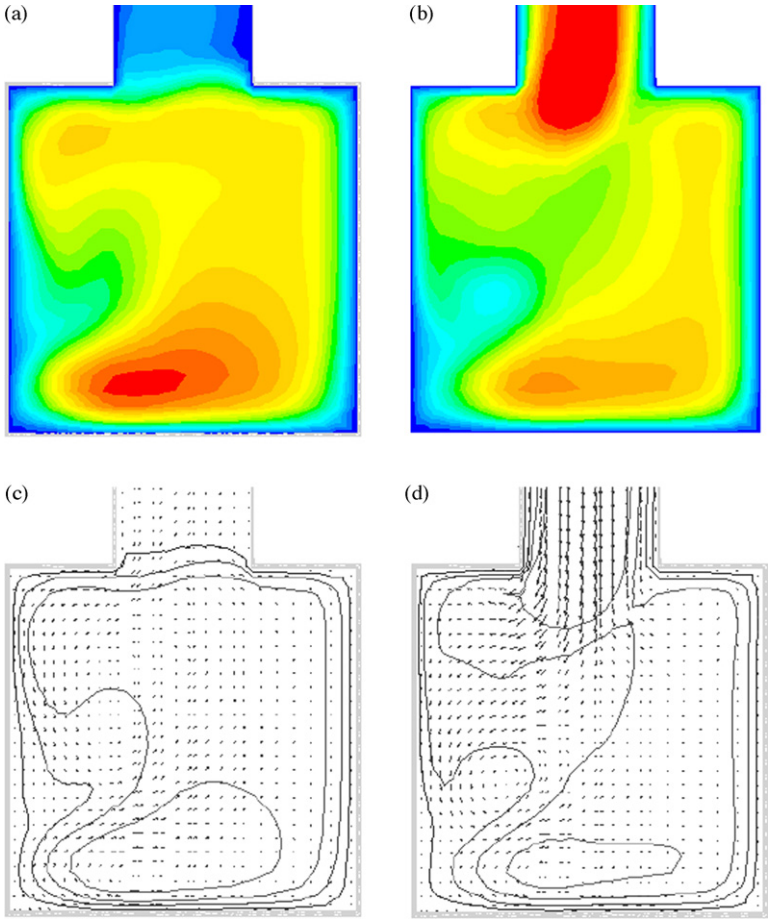

Fig. 13. Modification of the flow structure due to the feeding injection. Velocity contours inside the reactor for (a) 200 rpm, 180 ml h^{-1}, (b) 200 rpm, 7200 ml h^{-1}. Velocity vectors showing the flow disturbance (c) 200 rpm, 180 ml h^{-1}, (d) 200 rpm, 7200 ml h^{-1}.

5. Conclusions

The characterization of the flow-field in a torus reactor was carried out for two different configurations, batch and continuous reactor. In batch conditions, a linear evolution of the mean circulation velocities with respect to the impeller rotation speed was obtained, as it was already determined by Belleville et al. [8] for a circular-sectioned torus reactor. The mixing time values obtained in all hydrodynamic conditions were short, less than 21 s in all studied cases, to achieve a rapid concentration homogeneity into the reactor. The dimensionless mixing time was determined and was found to be independent of the Reynolds number when the impeller rotation speed is greater than 1200 rpm ($Re > 5800$). Thus, fully turbulent regime should be obtained into the torus reactor from these values of Reynolds number, achieved from $N =$ 1200 rpm.

In continuous mode, the torus reactor can exhibit a more complex behaviour, due to the perturbation of the inside flow by the feeding injection (acceleration or deceleration of the flow circulation in the reactor). This was shown for particular conditions of impeller rotation speeds and feeding flow rates. For common operating conditions, the hydrodynamics is however mainly a function of the impeller rotation speed. Further study will quantify influence of such perturbation in the case of enzymatic conversion using the torus reactor in continuous regime.

Acknowledgements

Special thanks to the Spanish Ministerio de Educación y Ciencia for the concession of the “Acción Integrada Franco-Española ref.: HF2003-0003” that financed all the displacements to Nantes (France) to carry out part of this research work.

Laura Pramparo is indebted to the Universitat Rovira i Virgili and Agència de Gestió d’Ajuts Universitaris i de Recerca (AGAUR) of Catalan Government for providing a pre-doctoral scholarship.

Special thanks to the Grup de Recerca en Experimentació, Computació i Modelització en Mecànica de Fluids i Turbulència (Mechanical Department of Universitat Rovira i Virgili) for providing the utilization of their equipment (commercial code Fluent Inc.).

Christophe Bengoa thanks Ramón y Cajal programme of Spanish Ministerio de Educación y Ciencia for its financial support.

References

[1] L. Nouri, J. Legrand, Y. Popineau, P. Belleville, Enzymatic hydrolysis of wheat proteins. Part II. Comparison of performance of batch-stirred and torus reactors, Chem. Eng. J. 65 (1997) 195–199.

[2] Y. Sato, Flow pattern, circulation velocity and pressure loss in loop reactor, J. Chem. Eng. Japan 12 (1979) 448–453.

[3] J. Legrand, J. Guéguen, S. Bérot, Y. Popineau, L. Nouri, Acetylation of pea isolate in a torus microreactor, Biotech. Bioeng. 53 (1997) 409–414.

[4] H. Benkhelifa, C. Bengoa, C. Larre, E. Guibal, Y. Popineau, J. Legrand, Casein hydrolysis by immobilized enzymes in a torus reactor, Proc. Biochem. 40 (2005) 461–467.

[5] K. Hosogai, M. Tanaka, Study of suspension polymerisation of styrene with a circular loop reactor, Polym. Eng. Sci. 32 (1992) 431–437.

[6] H. Laederach, F. Widmer, Le bioréacteur torique, Inf. Chim. 249 (1984) 157–160.

[7] I. Adler, A. Fiechter, Valuation of bioreactors for low viscous media and high oxygen transfer demand, Bioprocess. Eng. 1 (1986) 51–59.

[8] P. Belleville, L. Nouri, J. Legrand, Mixing characteristics in the torus reactor, Chem. Eng. Technol. 15 (1992) 282–289.

[9] A. Khalid, J. Legrand, J.M. Rosant, Turbulent flow induced by an impeller in a closed toroidal loop, J. Fluids Eng. 118 (1996) 677–684.

[10] A. Khalid, J. Legrand, Energy dissipation distribution and mixing in a torus reactor, Chem. Eng. Commun. 185 (2001) 141–164.

[11] J. Legrand, P. Belleville, Flow characteristics and transport phenomena in toroidal loop reactors, Chem. Eng. Technol. 25 (6) (2002) 667–670.

[12] H. Benkhelifa, J. Legrand, P. Legentilhomme, A. Montillet, Study of the hydrodynamic behaviour of the batch and continuous torus reactors in laminar and turbulent flow regimes by means of tracer methods, Chem. Eng. Sci. 55 (2000) 1871–1882.

[13] K. Kataoka, H. Doi, T. Komai, Heat/mass transfer in Taylor vortex flow with constant axial flow rates, Int. J. Heat Mass Transfer 20 (1977) 57–63.

[14] J. Pruvost, J. Legrand, P. Legentilhomme, Numerical investigation of bend and torus flows. Part I. Effect of swirl motion on flow structure in U-bend, Chem. Eng. Sci. 59 (2004) 3345–3357.

[15] J. Pruvost, J. Legrand, P. Legentilhomme, J.M. Rosant, Numerical investigation of bend and torus flows. Part II. Flow simulation in torus reactor, Chem. Eng. Sci. 59 (16) (2004) 3359–3370.

[16] J. Pruvost, L. Pottier, J. Legrand, Numerical investigation of hydrodynamic and mixing conditions in a torus photobioreactor, Chem. Eng. Sci. 61 (2006) 4476–4489.

[17] A. Brucato, M. Ciofalo, F. Grisafi, G. Micale, Numerical prediction of flow-fields in baffled stirred vessels: a comparison of alternative modelling approaches, Chem. Eng. Sci. 53 (21) (1998) 3653–3684.

[18] D.C. Wilcox, Turbulence Modelling for CFD, DCW Industries, Inc., La Canada, California, 1998.

[19] N. Harnby, M. Edwards, A. Nienow, Mixing in the Process Industries, Butterworth Heinemann, London, 1997.